

Supporting online information

Modular design of highly active unitized reversible fuel cell electrocatalysts

Malte Klingenhof,¹ Philipp Hauke,¹ Sven Brückner,¹ Sören Dresp,¹ Elisabeth Wolf,² Hong Nhan Nong,^{1,3} Camillo Spöri,¹ Thomas Merzdorf,¹ Denis Bernsmeier,¹ Detre Teschner,^{2,3} Robert Schlögl,^{2,3} Peter Strasser^{1*}

1. The Electrochemical Energy, Catalysis, and Materials Science Laboratory, Department of Chemistry, Chemical Engineering Division, Technical University Berlin, Berlin, Germany

2. Fritz Haber Institute of the Max Planck Society, Department of Inorganic Chemistry, Faradayweg 4, D-14195 Berlin, Germany

3. Max Planck Institute for Chemical Energy Conversion, Department of Heterogeneous Reactions, Stiftstr. 34-36, D-45470, Mülheim an der Ruhr, Germany

Corresponding author:

Peter Strasser, e-mail: pstrasser@tu-berlin.de;

Experimental Section

Regular Characterization

- Figure S1:** Scheme of the synthesis of the ORR catalyst and Cu- α -MnO₂ (a - b) and the OER catalyst NiFe-LDH (c - d)..... 5
- Figure S2:** Schematic depiction of the modification step leading to O-modified carbon support materials. 6
- Figure S3:** Scheme of the MCPT setup..... 9
- Figure S4:** XPS spectra of Cu- α -MnO₂/XC-72R/NiFe-LDH. F 1s results from binder material..... 10
- Figure S5:** XRD pattern of (003) diffraction reflection NiFe-LDH before and after anion exchange a). The successful anion exchange is confirmed by a shift of the diffraction reflection of the (003) peak to lower values of 2θ 11
- Figure S7:** TEM images of different carbon support materials, which are investigated in this publication. The scale bar of the upper row is 20 nm and the scale bar of the lower row is 10 nm. The different carbon support materials show the expected morphological features. Despite MWCNTs the appearance of the different types of carbon show only negligible differences. 11
- Figure S7:** Comparison of BET a) and XRD diffraction b) measurements of different carbon support materials. XRD diffraction patterns of the different carbon support materials show the common carbon diffraction reflections. BET investigations reveal different physical surface areas of the carbon support materials. Ketjen Black reveals the highest and C₆₅ the lowest surface area. 12
- Figure S8:** BET (a) and XRD (b) investigations of the oxygen modified MWCNTs. The surface area is increasing with increasing exposure time to the oxidative environment. The crystal structure is slightly affected by the oxygen modification, evident by the decreasing diffraction reflections. 12
- Figure S9:** XPS measurements of oxygen modified MWCNTs with different oxidation times. a-c) C1s spectra, d-f) O1s spectra and g-i) survey. XPS measurements show that the electronic surface state of the prepared materials are not affected by the oxygen modification. 13
- Figure S10:** Investigations of the electrocatalytic activity towards OER using modified NiFe-LDH supported on MWCNTs. a) LSV curves measured in N₂ saturated 0.1 M KOH at RT and 1600 rpm. Addition of support materials to the NiFe-LDH increases the accessible surface area of each material and increases the electrocatalytic activity accompanied by increase of activity with modification. b) Potential (vs. RHE) necessary to provide a current density of 10 mA cm⁻². 14
- Figure S11:** Electrochemical investigation of carbon-based support materials. a) ORR activity of the carbon support materials. b) OER activity of the carbon support materials. Changing the applied carbon-based support materials improves the electrochemical properties in case of ORR and OER. Ketjen Black is the best catalyst support for ORR type catalysts and MWCNTs for OER type catalysts. The measurements were conducted in O₂ saturated 0.1 M KOH at 1600 rpm and RT. 15
- Figure S12:** Investigations of O-modified MWCNTs: a) LSV curves of oxygen modified MWCNT after different reaction times compared to unmodified MWCNTs. b) Comparison of physical surface area measured with BET and electrochemical accessible surface area (ECSA). c) Comparison of the initial ECSA of the O-MWCNTs with the ECSA after stability testing. d) Comparison of the initial ORR/OER activity with the remaining activity after stability testing. Modifying MWCNTs with oxygen improves the performance of the MWCNTs towards ORR and OER. O-2h turned out to be the best material despite lower BET surface area. 16
- Figure S13:** Influence of 0.5 M NaCl on the electrocatalytic activity of Cu- α -MnO₂/XC-72R/NiFe-LDH. a) Determination of the electrocatalytic activity towards ORR and OER in the presence of 0.5 M NaCl. b)

Galvanostatic stability investigations of the catalyst in the presence of 0.5 M NaCl solution (red line). The measurements were conducted like reported for 0.1 M KOH. 16

Figure S14: Change of the electrocatalytic activity of Cu- α -MnO₂/XC-72R/NiFe-LDH (black and grey) and Pt-C/Ir-C (both 20 wt. % at C) (dashed blue and dashed light blue). a) OER activity before and after galvanostatic stability testing. b) ORR activity before and after galvanostatic stability testing. c) and d) SEM images an electrode consisting of Cu- α -MnO₂/XC-72R/NiFe-LDH after exposure to bias. 17

Figure S15: Comparison of two different URFC testing sequences. a) Alternating fuel cell (FC) and water electrolysis (WE) mode, starting with FC. b) Alternating FC and WE testing starting with WE. For the depicted measurements commercial reference catalysts (Pt-C/Ir-C, both 20 wt% at C) were used. 0.1 mgPt cm⁻² at the hydrogen electrode and 2.0 mgCat. cm⁻² on the oxygen electrode. 2.0 mgCat. cm⁻² corresponds to an overall catalyst loading of Pt-C/Ir-C (20 wt. % at XC-72R), including XC-72R. Based on the experience and results of the measurements, the sequence FC-WE was applied to the following measurements..... 17

Figure S16: Decrease of current density within the first three polarization curves at high potentials. a) Decrease of current density over three URFCs measurement cycles. b) Decrease in current density occurring during the first three polarization curves. The measurements were conducted using Cu-a-MnO₂/XC-72R/NiFe-LDH (2.5 mg cm⁻²) as the oxygen electrode and Pt-C (46.7 wt. %, TKK, 0.1 mg Pt cm⁻²) as the hydrogen electrode. The fuel cell measurements were conducted with a Hydrogen flow of 250 mL hr, an Oxygen flow of 500 mL hr with a RH (relative humidity) of 100. WE (Water electrolysis) measurements were carried out in 0.1 M KOH at 50 °C. 18

Experimental Section

Catalyst preparation

Synthesis of NiFe-LDH and Cu- α -MnO₂ (α -MnO₂). The synthesis of NiFe as layered double hydroxide (LDH) with molar Nickel : Iron ratio of 5 : 1 was prepared using a microwave assisted one-pot synthesis described by Dresp *et al.*¹ 1200 μ L of 0.6 M Ni(OAc)₂*4H₂O and 240 μ L of 0.6 M Fe(NO₃)₃*9 H₂O precursor solution were added to 6 mL DMF and stirred subsequently. 4 mL DMF and 8 mL ultrapure water were added. The resulting solution was transferred to a microwave and reacted with constant stirring for 60 min at 120 °C and 160 °C for 30 min. The product was collected, washed with ethanol and Mili-Q and finally dried in a freeze dryer. NiFe-LDH resulted in a Ni/Fe ratio of 3.25 ± 0.07 .

α -MnO₂ was synthesized by a top-down approach described by Ding *et al.*² In a typical experiment 0.1 mol KMnO₄ and 0.15 mol Mn(OAc)₂*4H₂O were mixed and ground in a ball miller. The mixture was kept in an oven at 120 °C for 4 h. The resulting black powder, was washed by sonication and centrifugation with ultrapure water for several times and finally dried at 80 °C in air over night. For the synthesis of copper doped α -MnO₂, the CuCl₂ was added in the desired ratio directly into the ball miller. The synthesis was continued as described above. The amount of copper in Cu- α -MnO₂ was found to be 3.42 ± 0.16 wt. %, which corresponds to the used amount of copper.

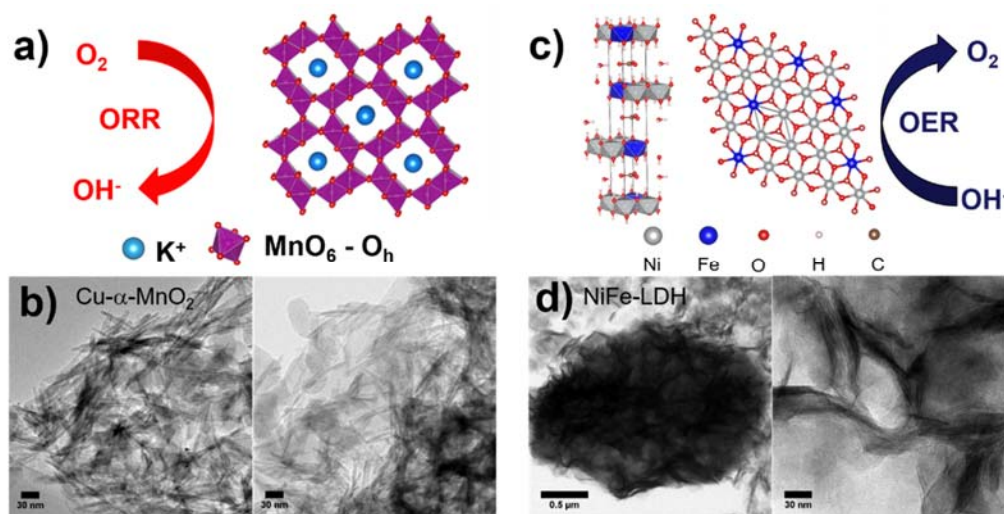


Figure S1: Scheme of the synthesis of the ORR catalyst and $Cu-\alpha-MnO_2$ (a - b) and the OER catalyst NiFe-LDH (c - d).

Modification of NiFe-LDH. The modification of NiFe-LDH was conducted based on an anion exchange via Cl^- and ClO_4^- described by Song *et al.*³ Anion exchange for chloride was carried out by mixing 100 mg of the NiFe-LDH powder with 100 ml of the saturated salt solution (NaCl) and 100 ml of HCL (0.01 M). The reaction mixture was stirred mechanically at RT, over 24 h at 600 rpm. The resulting product was collected by centrifugation washed with Milli-Q, EtOH and finally dried by lyophilization. Anion exchange for perchlorate was carried out by mixing 100 mg of the NiFe-LDH- Cl^- powder with 100 ml of the saturated salt solution ($NaClO_4$) and 100 ml of HCL (0.01 M). The reaction mixture was stirred mechanically at RT, over 18 h at 600 rpm. The resulting product was collected by centrifugation washed with H_2O , ETOH, H_2O and was finally dried by lyophilization.

Modification of multi walled carbon nanotubes (MWCNTs). Based on electrochemical evaluations of different carbon support materials multi walled carbon nanotubes (MWCNTs) were used for the following modification step. The electrochemical evaluations are depicted in Figure (Figure S11). O-Modification strategies of carbon materials are schematically depicted in Figure S2 schematically.

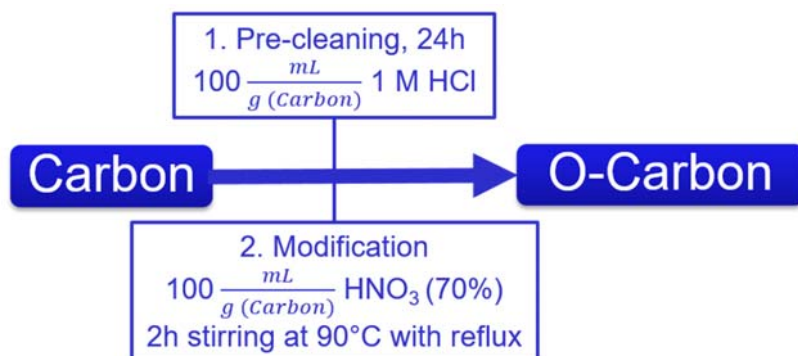


Figure S2: Schematic depiction of the modification step leading to O-modified carbon support materials.

One gram unmodified MWCNTs were purified in 100 mL diluted HCl (1 M, 70 ml ultrapure water and 30 ml 37% HCl) for 24 h at RT to remove leftover metals. Afterwards, the MWCNTS were washed with ultrapure water, until a neutral pH was reached. The resulting carbon was collected in a round bottom flask and treated with 100 mL HNO₃ (69 %) for 2 h at 90 °C. The flask was purged with N₂ to remove the remaining NO_x. Afterwards, the carbon was washed with deionized water to adjust pH 7. The product was dried via lyophilisation for 12 h. The resulting samples got the prefix O and the suffix dependence on the duration in HNO₃ as example O-2h. The oxygen, which is added to the carbon structure, will modify the electronic structure. Through the higher electronegativity of the oxygen, the adjacent carbon change their electronic structure too and improve the OER intermediates and therefore the OER process. Additional, COOH and C-O-C groups improve the ORR reaction through an efficiently reduction of O₂ to HO₂ intermediates.

Physicochemical characterization

X-Ray diffraction patterns were measured using a Bruker D8 Advance X-Ray Powder diffractometer equipped with a Lynx Eye detector and Kf1 Cu 2k X-Ray tube in step scan mode with a scanning rate of 0.006 ° in the 2θ range from 10 ° to 80 °. The elemental composition was determined using inductively coupled plasma optical emission spectroscopy (ICP-OES) with a 715-ES-inductively coupled plasma analysis system (Varian). Transmission electron microscope (TEM) measurements were conducted using a Tecnai G2 20 s-Twin microscope, equipped with a LaB₆-cathode and a GATAN MS794 P CCD-detector at ZELMI Centrum, Technical University of Berlin. TEM samples were ultrasonicated in *i*-PrOH and drop-dried on copper grids. Scanning

electron microscope (SEM) measurements were carried out with a JOEL 7401F instrument with an accelerating voltage of 10 kV. The zeta potentials of the particles were measured using a Malvern Instruments Zeta Sizer Nano. XPS measurements of the catalysts and reference materials, were performed at FHI using nonmonochromatized Mg K α (1486.6 eV) excitation and a hemispherical analyzer (Phoibos 150, SPECS). The measured spectra were analysed by using CasaXPS.

Electrochemical evaluation with RDE setup

For electrocatalytic activity testing, a catalyst suspension was prepared. The suspension consists of 4 mg catalyst, 768 μ L DI water, 200 μ L *i*-PrOH and 32 μ L 5 wt. % Nafion perfluorinated resin solution (Sigma Aldrich). 10 μ L of the resulting dispersion was pipetted on the GC electrode. The electro-catalytic performance of the catalyst was evaluated in O₂-saturated 0.1 M KOH at 1600 rpm using a Biologic SP-200 potentiostat operating in a three-electrode setup with a platinum counter electrode (CE) and a reversible hydrogen (RHE) reference electrode. All reported CVs were IR and capacity corrected. The overpotentials reported, necessary to reach a current density of 10 mA cm⁻² (OER) and -3 mA cm⁻² (ORR) are the average of three measurements. Stability measurements of the multi-component system were conducted with the same setup. 24 h hours galvanostatic stability measurements were conducted to periodically evaluate ORR and OER performance at -3 mA cm⁻² (ORR) and 4 mA cm⁻² (OER) starting with ORR and changing between ORR and OER hourly.

Microwave cavity perturbation technique (MCPT)

Contact-free measurements of the electrical conductivity were performed with microwave cavity perturbation technique (MCPT) described by Eichelbaum *et al.*⁴ Measurements of the conductivity is based on the perturbation of incident microwaves by a conducting sample. The TM₀₁₀ mode of a cylindrical silver and gold plated copper S-band cavity with a height of 20 mm and a radius of 34 mm was used with a resonance frequency of 3.2 GHz.⁵ A quartz tube reactor with 4 mm outer diameter and 3 mm inner diameter containing the sample was directly placed in the center of the cavity. The sample with an overall length of 10 mm was fixed with two quartz wool plugs. A 10 mm outer diameter double-walled evacuated quartz Dewar surrounds the sample containing reactor, to protect the resonator from convection heat and to enable heating using a pre-

heated nitrogen flow. While the sample was preheated to 50 °C, the resonator was kept at 20 °C. Temperature control is ensured via a thermometer placed in the reactor without affecting the microwave. The flow of dried N₂ (15 mL min⁻¹) further prevented water condensation within the resonator. A scheme of the used setup is depicted in Figure S3. The data were fitted using a Matlab-based algorithm by Kajfez.⁶

Investigation of the electrical conductivity is based on a perturbation of the resonator properties of a microwave cavity by the electrocatalyst leading to a decrease of the resonator Q factor and resonant angular frequency ω . These perturbations can be related to changes of the relative complex permittivity $\varepsilon = \varepsilon' - i\varepsilon''$ describing the response of the samples to the electric field component of the microwave. $\varepsilon' - i\varepsilon''$ can be calculated via equation 1 and 2.⁷

$$B\varepsilon_p'' \frac{V_s}{V_c} = \frac{1}{Q_s} - \frac{1}{Q_0} \quad eq. 1$$

$$A(\varepsilon_p' - 1) \frac{V_s}{V_c} = \frac{(\omega_0 - \omega_s)}{\omega_s} \quad eq. 2$$

$$\sigma = \varepsilon_0 \omega_s \varepsilon'' \quad eq. 3$$

V: Volume (Subscript *S*: Sample; *C*: Cavity)

ω : resonant angular frequency (Subscripts *S* and *0* refer to the cavity with sample (*S*) and without sample (*0*))

A and *B*: Calibration constants of the resonator and the microwave

Q: resonant factor

ε' and ε'' : real and imaginary part of the relative complex permittivity (Subscript *P* refers to the permittivity of the powder and subscript *0* refers to the permittivity of the vacuum)

The resulting powder permittivities (ε_p) were corrected to bulk values using formulae resulting from effective medium theory.^{8,9} The conductivity was then calculated using equation (eq. 3) reported in Wernbacher *et al.*⁷

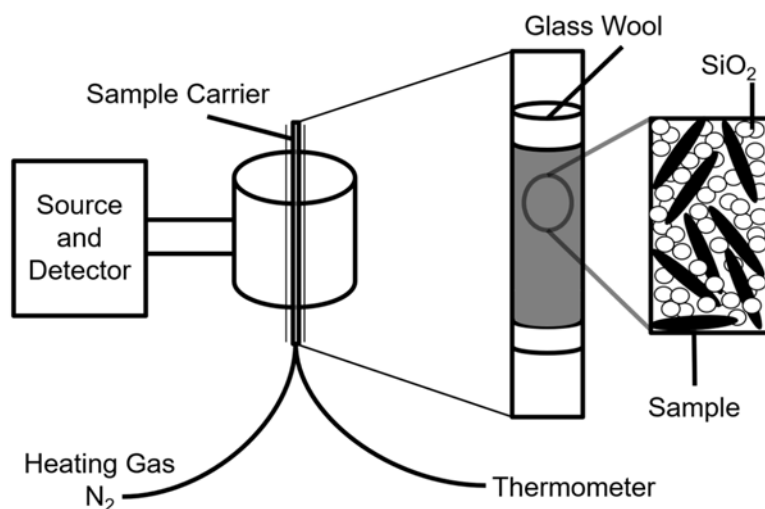


Figure S3: Scheme of the MCPT setup.

The sample preparation was conducted by diluting the sample of interest with SiO₂ nano powder. For this purpose, a dilution series was produced evaluating the optimal measurement range, this is necessary since the measurement is designed for the evaluation of semi-conducting samples. α -MnO₂/SiO₂ mixtures were produced in ratios of 1/1, 1/10, 1/20, 1/50 and 1/100. The ideal measuring range is a α -MnO₂/SiO₂ ratio of 1/20. The different M- α -MnO₂ (M = -, Co, Ni, Cu) samples were then produced and measured using this ratio. α -MnO₂ was used for the dilution series. The samples were prepared by mixing the necessary quantities of SiO₂ and M- α -MnO₂ with a mortar, using a total sample quantity of 100 mg preparing the desired M- α -MnO₂/SiO₂ ratio.

MEA preparation for URFC full cell measurements

(Tokuyama A201 Membrane, AS-4 Tokuyama Ionomer) The membrane electrode assembly (MEA) was prepared by manual spray coating technique. For spray coating the membrane was fixed on a commercial heating vacuum plate equipped with temperature control (Carbon and Fuel Cell) and a dry vacuum pump/compressor (Welch, WOB-L 2511). The table temperature was set to 55 °C. Furthermore, a mask (5 cm²) was used to ensure vis-a-vis coating of anode and cathode side catalyst. The used ink consisted of 50 mg catalyst powder, 50 μ L ultrapure water (18.2 M Ω cm⁻²), 3 mL *i*-PrOH and 460 mg ionomer (AS-4, Tokuyama, AS-4, 15 wt. % solution in water). Typically, 650 μ L ink was sprayed on the membrane, aiming at a Pt loading of 0.1 mg cm⁻² at the hydrogen side. For the oxygen electrode an overall catalyst loading of 2.0 mg cm⁻² is adjusted,

including carbon support materials. After spray coating, the as prepared CCM was dried for ten minutes at 55 °C followed by cooling to RT and weighing. To achieve a satisfying loading spraying and weighting step were carried out several times with low amounts of the catalyst ink. The measurement was carried out in a unitized regenerative fuel cell (URFC) setup. The setup consists of the prepared membrane, furthermore oxygen and hydrogen side are equipped with gaskets, porous transport layers (PTL), endplates with gas respectively electrolyte ports, bi-potential plates (serpentine flow fields, carbon plate for the hydrogen side and gold coated titanium plate for the oxygen side). In case of the URFC sequence 4 x FC-WE (starting with fuel cell mode) the CCMs were pretreated based on a protocol described by Eriksson *et al.*¹⁰ To achieve the best performance the spray-coated CCMs were anion-exchanged in 1 M KOH three times, each 20 min. To remove remaining surplus OH⁻ the anion-exchanged membrane was washed with DI water (18.2 MΩ cm⁻²) three times for 20 min. Before evaluating the activity, the CCM was activated by two potential steps (1 h at 0.5 V and 15 min at 0.2 V). In case of the URFC sequence WE-FC (starting with WE mode) the prepared CCM were directly built into the electrochemical cell, only an electrochemical conditioning was performed.

Results of the physicochemical characterization

Investigation of Cu- α -MnO₂/XC-72R/NiFe-LDH.

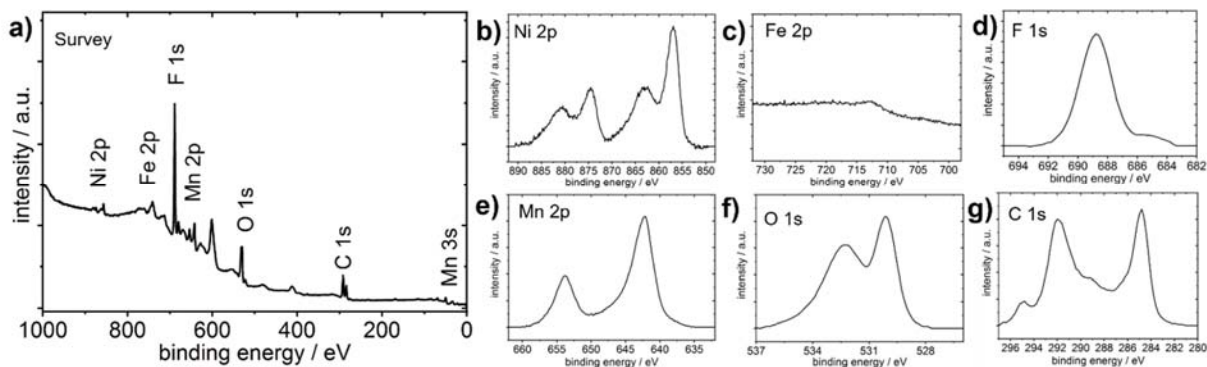


Figure S4: XPS spectra of Cu- α -MnO₂/XC-72R/NiFe-LDH. F 1s results from binder material.

Investigation of the modified NiFe-LDH.

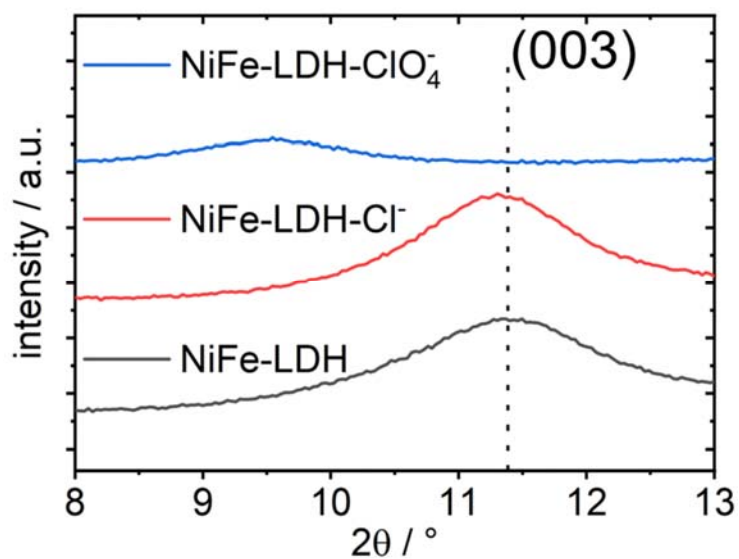


Figure S5: XRD pattern of (003) diffraction reflection NiFe-LDH before and after anion exchange a). The successful anion exchange is confirmed by a shift of the diffraction reflection of the (003) peak to lower values of 2θ .

Investigations of tin oxide and carbon-based support materials.

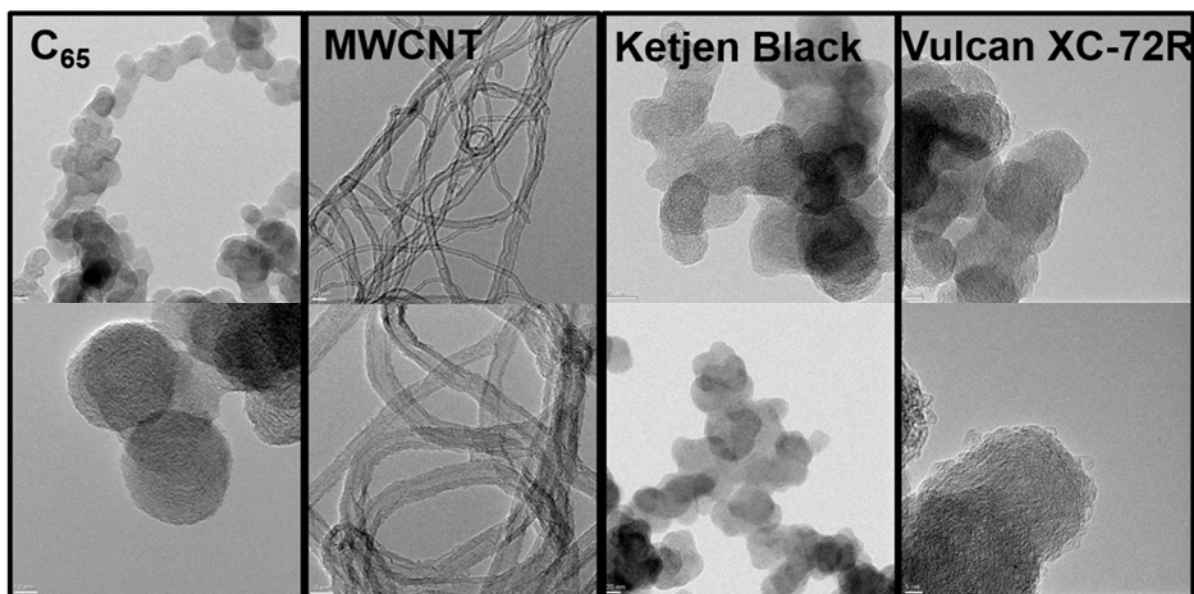


Figure S6: TEM images of different carbon support materials, which are investigated in this publication. The scale bar of the upper row is 20 nm and the scale bar of the lower row is 10 nm. The different carbon support materials show the expected morphological features. Despite MWCNTs the appearance of the different types of carbon show only negligible differences.

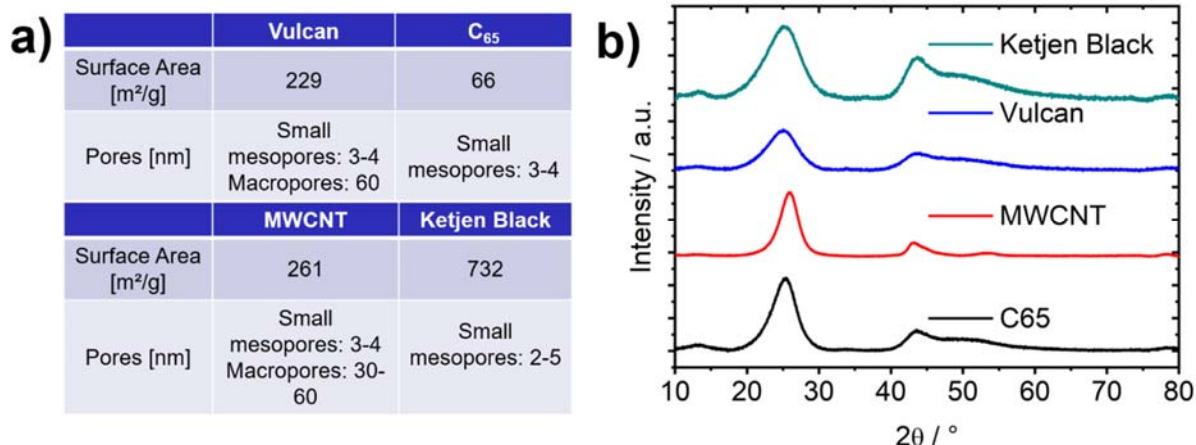


Figure S7: Comparison of BET a) and XRD diffraction b) measurements of different carbon support materials. XRD diffraction patterns of the different carbon support materials show the common carbon diffraction reflections. BET investigations reveal different physical surface areas of the carbon support materials. Ketjen Black reveals the highest and C₆₅ the lowest surface area.

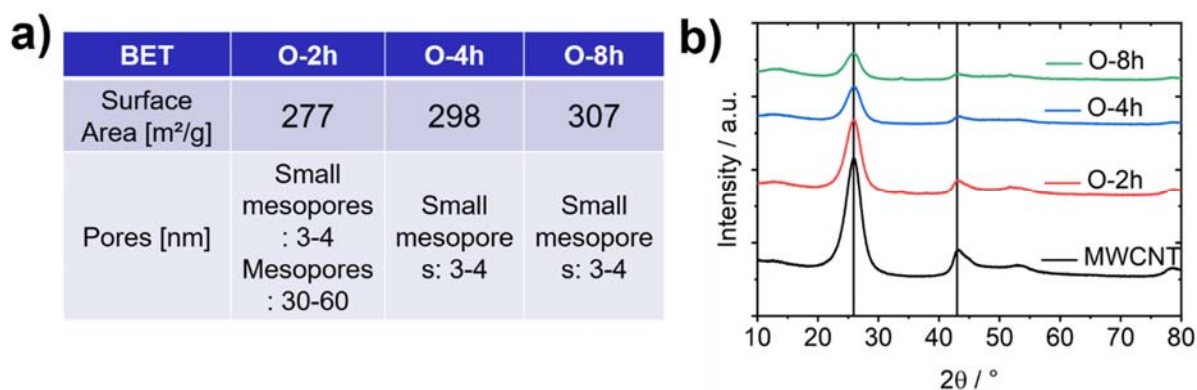


Figure S8: BET (a) and XRD (b) investigations of the oxygen modified MWCNTs. The surface area is increasing with increasing exposure time to the oxidative environment. The crystal structure is slightly affected by the oxygen modification, evident by the decreasing diffraction reflections.

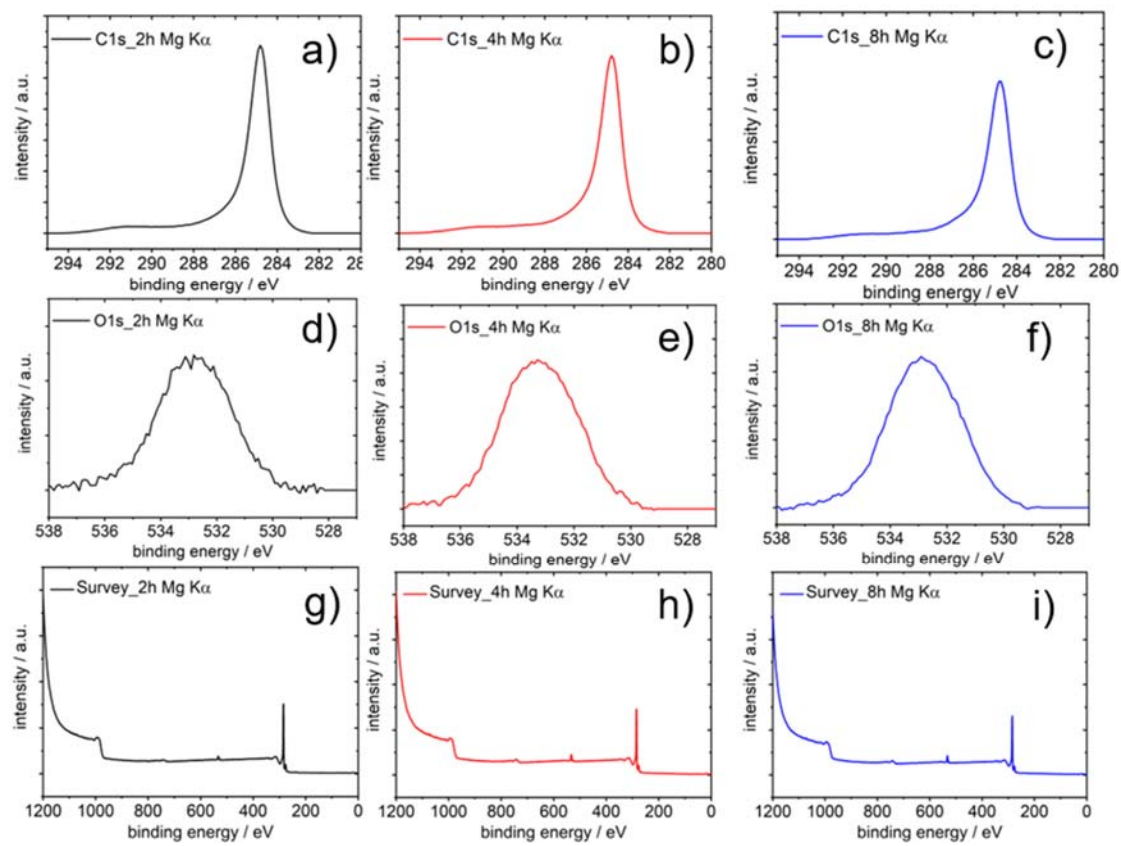


Figure S9: XPS measurements of oxygen modified MWCNTs with different oxidation times. a-c) C1s spectra, d-f) O1s spectra and g-i) survey. XPS measurements show that the electronic surface state of the prepared materials are not affected by the oxygen modification.

Results of the electrochemical investigation

Investigation of NiFe-LDH.

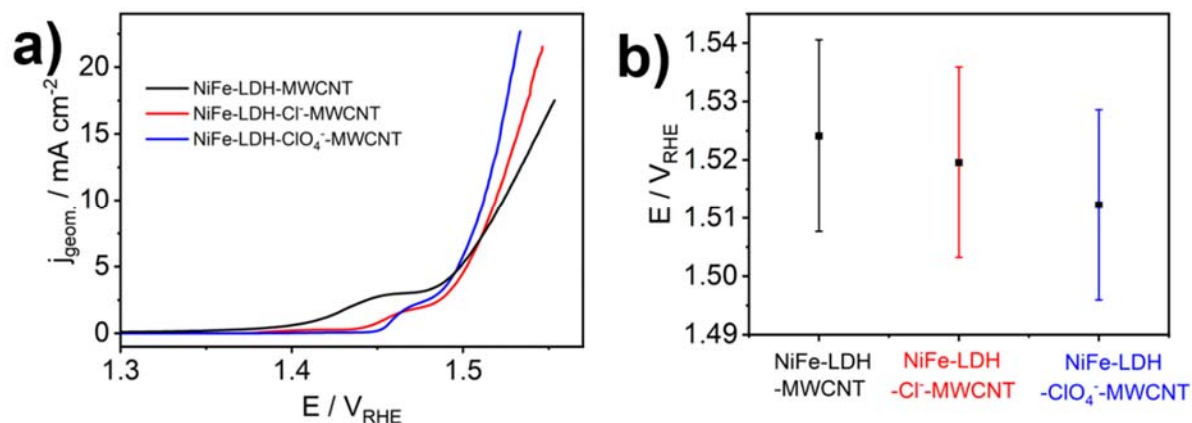


Figure S10: Investigations of the electrocatalytic activity towards OER using modified NiFe-LDH supported on MWCNTs. a) LSV curves measured in N_2 saturated 0.1 M KOH at RT and 1600 rpm. Addition of support materials to the NiFe-LDH increases the accessible surface area of each material and increases the electrocatalytic activity accompanied by increase of activity with modification. b) Potential (vs. RHE) necessary to provide a current density of 10 mA cm^{-2} .

Investigations of carbon-based support materials

Electrochemical evaluation of tin oxide and carbon-based support materials.

Table S1: Protocols of the electrochemical evaluation of the support materials.

ECSA	Activity	Stability
15 min N_2	15 min O_2	15 min N_2
CA, 0.6 V, 1 min	CA, 0.6 V, 1 min	CA, 0.35 V, 50 s
CV, 0.6 V -1.6 V, 50 mV/s, 20 cycles	CV, 0.4 V - 1.1 V, 5 mV/s, 2 cycles	CA, 0.35 V, 5 s
PEIS, 0.6 V, 100,000 Hz - 1 Hz	CV, 0.6 V - 1.1 V, 50 mV/s, 21 cycles	CV, 0.4 V -1.8 V, 5 mV/s, 2 cycles
OCV, 2min	CV, 0.4 V - 1.1 V, 5 mV/s, 2 cycles	PEIS, 1 V, 100,000 Hz - 1 Hz
CVA, OCV \pm 0.05 V, 500 mV/s; 250 mV/s; 125 mV/s; 60 mV/s; 30 mV/s; 15 mV/s; 5 mV/s, 3 cycles for each rate	PEIS, 1 V, 100,000 Hz - 1 Hz	CV, 0.4 V -1.8 V, 500 mV/s, 1000 cycles

PEIS, at OCV, 100,000 Hz – 1 Hz CA, 0.4 V, 5 s	CV, 1 V -1.8 V, 5 mV/s, 2 cycles CV, 1 V -1.8 V, 50 mV/s, 21 cycles	Loop, start at tech 2, 9 times CA, 0.6 V, 10 s
CV, 0.4 V – 1.1 V, 5 mV/s, 2 cycles CA, 1 V, 1 min	CV, 1 V -1.8 V, 5 mV/s, 2 cycles PEIS, 0.4 V, 100,000 Hz – 1 Hz CA, 1 V, 1 min	CV, 0.6 V -1.6 V, 50 mV/s, 20 cycles PEIS, 0.6 V, 100,000 Hz – 1 Hz OCV, 2min CVA, OCV \pm 0.05 V, 500 mV/s; 250 mV/s; 125 mV/s; 60 mV/s; 30 mV/s; 15 mV/s; 5 mV/s, 3 cycles for each rate PEIS, at OCV, 100,000 Hz – 1 Hz CA, 0.4 V, 5 s CV, 0.4 V – 1.1 V, 5 mV/s, 2 cycles CA, 1 V, 1 min

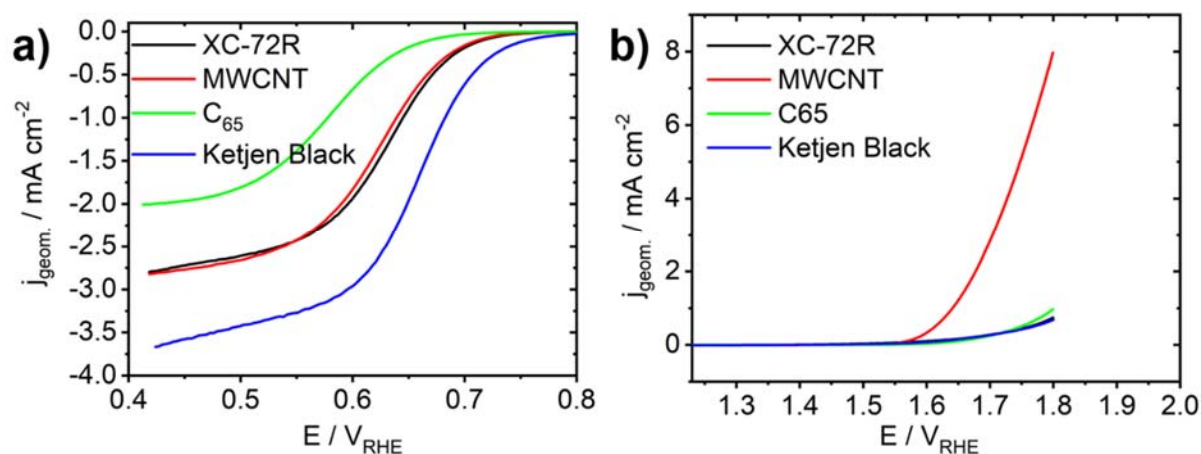


Figure S11: Electrochemical investigation of carbon-based support materials. a) ORR activity of the carbon support materials. b) OER activity of the carbon support materials. Changing the applied carbon-based support materials improves the electrochemical properties in case of ORR and OER. Ketjen Black is the best catalyst support for ORR type catalysts and MWCNTs for OER type catalysts. The measurements were conducted in O_2 saturated 0.1 M KOH at 1600 rpm and RT.

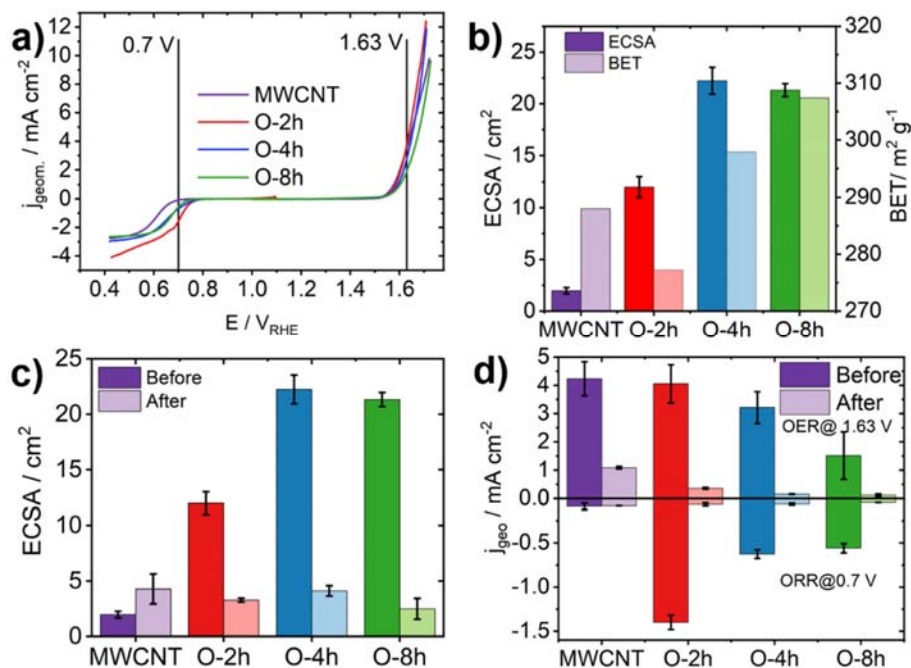


Figure S12: Investigations of O-modified MWCNTs: a) LSV curves of oxygen modified MWCNT after different reaction times compared to unmodified MWCNTs. b) Comparison of physical surface area measured with BET and electrochemical accessible surface area (ECSA). c) Comparison of the initial ECSA of the O-MWCNTs with the ECSA after stability testing. d) Comparison of the initial ORR/OER activity with the remaining activity after stability testing. Modifying MWCNTs with oxygen improves the performance of the MWCNTs towards ORR and OER. O-2h turned out to be the best material despite lower BET surface area.

Influence of NaCl on the electrocatalytic activity.

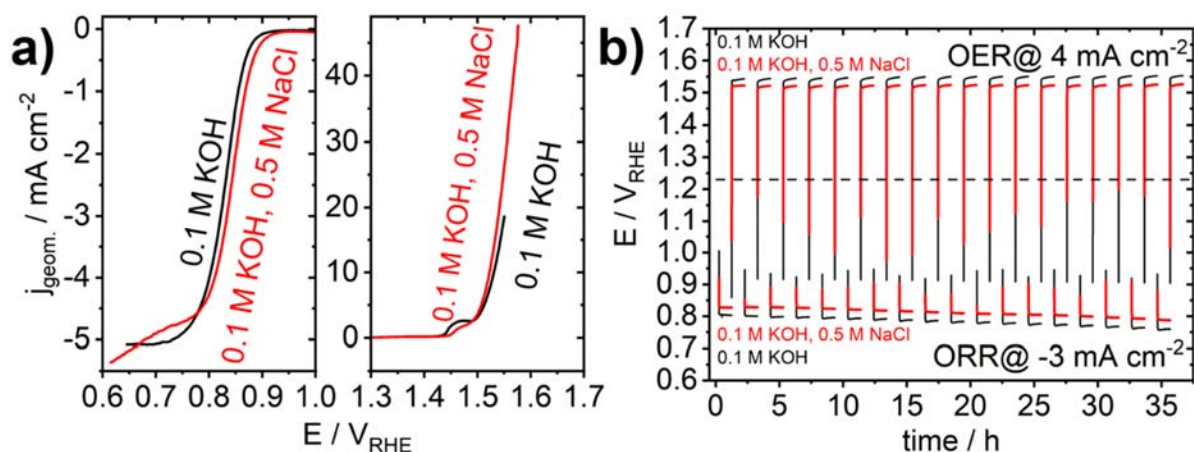


Figure S13: Influence of 0.5 M NaCl on the electrocatalytic activity of Cu- α -MnO₂/XC-72R/NiFe-LDH. a) Determination of the electrocatalytic activity towards ORR and OER in the

presence of 0.5 M NaCl. b) Galvanostatic stability investigations of the catalyst in the presence of 0.5 M NaCl solution (red line). The measurements were conducted like reported for 0.1 M KOH.

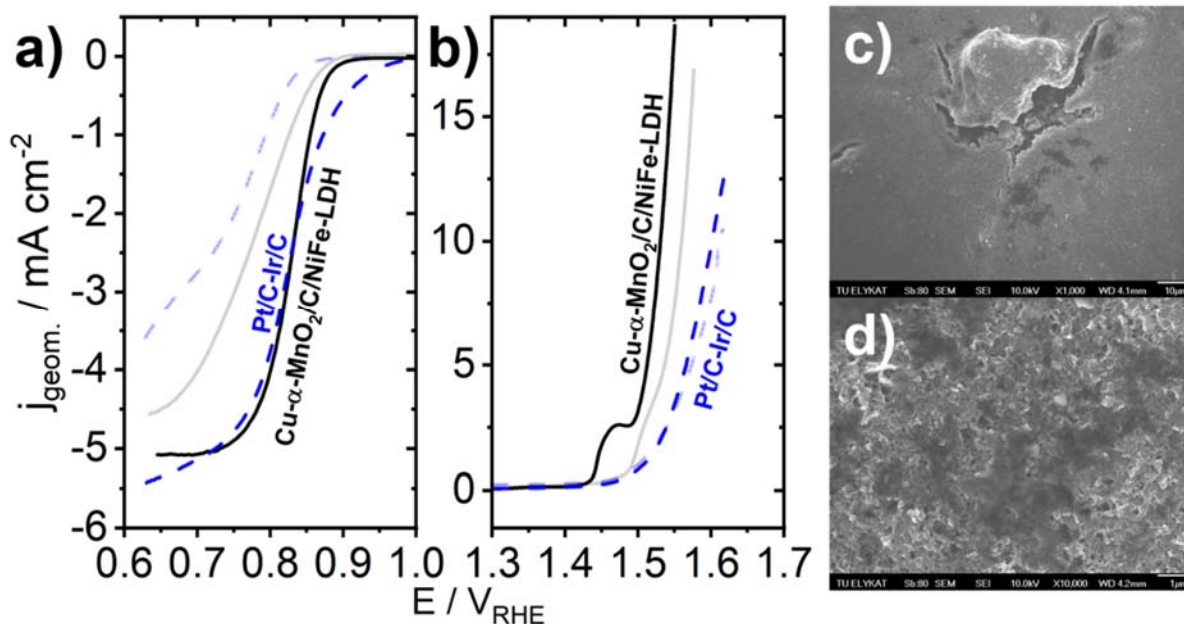


Figure S14: Change of the electrocatalytic activity of Cu- α -MnO₂/XC-72R/NiFe-LDH (black and grey) and Pt-C/Ir-C (both 20 wt. % at C) (dashed blue and dashed light blue). a) OER activity before and after galvanostatic stability testing. b) ORR activity before and after galvanostatic stability testing. c) and d) SEM images an electrode consisting of Cu- α -MnO₂/XC-72R/NiFe-LDH after exposure to bias.

MEA investigations

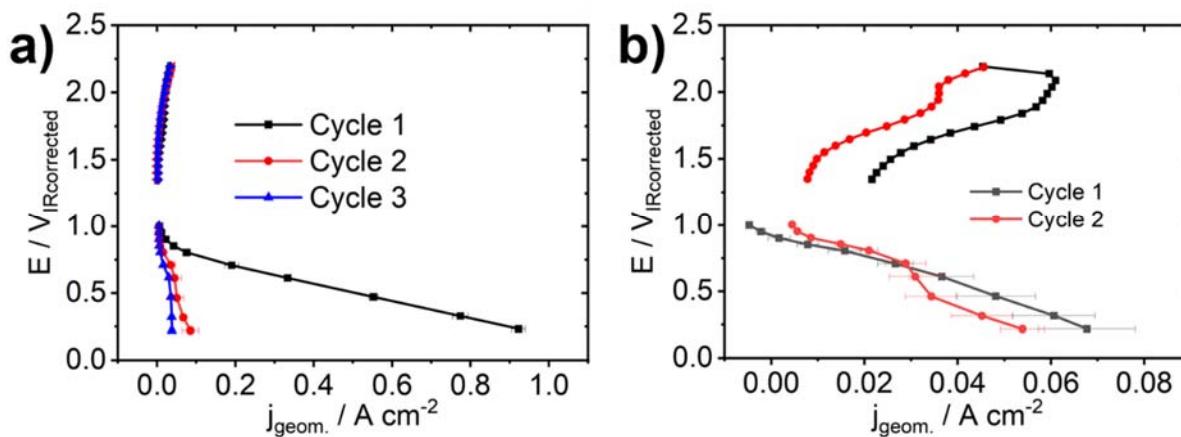


Figure S15: Comparison of two different URFC testing sequences. a) Alternating fuel cell (FC) and water electrolysis (WE) mode, starting with FC. b) Alternating FC and WE testing starting with WE.

with WE. For the depicted measurements commercial reference catalysts (Pt-C/Ir-C, both 20 wt% at C) were used. 0.1 mgPt cm^{-2} at the hydrogen electrode and $2.0 \text{ mgCat. cm}^{-2}$ on the oxygen electrode. $2.0 \text{ mgCat. cm}^{-2}$ corresponds to an overall catalyst loading of Pt-C/Ir-C (20 wt. % at XC-72R), including XC-72R. Based on the experience and results of the measurements, the sequence FC-WE was applied to the following measurements.

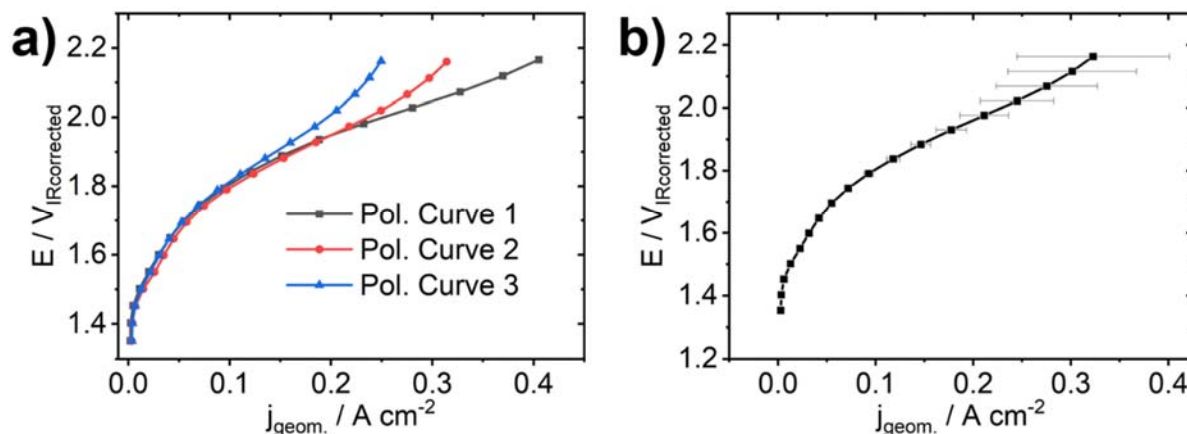


Figure S16: Decrease of current density within the first three polarization curves at high potentials. a) Decrease of current density over three URFCs measurement cycles. b) Decrease in current density occurring during the first three polarization curves. The measurements were conducted using Cu-a-MnO₂/XC-72R/NiFe-LDH (2.5 mg cm^{-2}) as the oxygen electrode and Pt-C (46.7 wt. %, TKK, $0.1 \text{ mg Pt cm}^{-2}$) as the hydrogen electrode. The fuel cell measurements were conducted with a Hydrogen flow of 250 mL hr , an Oxygen flow of 500 mL hr with a RH (relative humidity) of 100. WE (Water electrolysis) measurements were carried out in 0.1 M KOH at $50 \text{ }^\circ\text{C}$.

Table S2: Electrochemical protocols for URFC testing.

FC testing	WE testing
CA: 0.5 V , 1h	CV: 50 cycles, $1.1 \text{ V} - 1.7 \text{ V}$, 50 mV s^{-1}
CA: 0.2 V , 15 min	CA: 1.83 V , 1 h
PEIS: 0.5 V ,	PEIS: 1.6 V ,
MP: $1.0 \text{ V} - 0.2 \text{ V}$ 180 sec each, average over the last 20 sec.	MP: $1.3 \text{ V} - 2.2 \text{ V}$, 50 mV potential steps, 180 sec each, average over the last 20 sec.
Loop: Technique 3, 2 times	Loop: Technique 3, 2 times

Literature

- 1 Dresp, S. *et al.* An efficient bifunctional two-component catalyst for oxygen reduction and oxygen evolution in reversible fuel cells, electrolyzers and rechargeable air electrodes. *Energy & Environmental Science* **9**, 2020-2024, doi:10.1039/c6ee01046f (2016).

- 2 Yun-Shuan Ding *et al.* Synthesis and Catalytic Activity of Cryptomelane-Type Manganese
Dioxide Nanomaterials produced by a novel Solvent-Free Method. *Chem. Mater.* **17**, 5382-5389
(2005).
- 3 Song, F. & Hu, X. Exfoliation of layered double hydroxides for enhanced oxygen evolution
catalysis. *Nat Commun* **5**, 4477, doi:10.1038/ncomms5477 (2014).
- 4 Eichelbaum, M. *et al.* The microwave cavity perturbation technique for contact-free and in situ
electrical conductivity measurements in catalysis and materials science. *Phys Chem Chem Phys* **14**,
1302-1312, doi:10.1039/c1cp23462e (2012).
- 5 Heenemann, M. Charge Transfer in Catalysis Studied by In-situ MCPT. *Dissertation* (2017).
- 6 D.Kajfez. *Q factor Measurements Using Matlab (R)*. (Artech House Publishers, 2011).
- 7 Wernbacher, A. M. *et al.* Operando Electrical Conductivity and Complex Permittivity Study on
Vanadia Oxidation Catalysts. *The Journal of Physical Chemistry C* **123**, 8005-8017,
doi:10.1021/acs.jpcc.8b07417 (2018).
- 8 Dube, D. C. Study of Landau -Lifshitz-Looyenga's Formula for Dielectric Correlation Between
Powder and Bulk. *Journal of Physics D Applied Physics*, 1648-1652 (1970).
- 9 Looyenga, H. Dielectric Constants of Heterogeneous Mixtures. *Physica* **31**, 401-406 (1965).
- 10 Eriksson, B. *et al.* Quantifying water transport in anion exchange membrane fuel cells.
International Journal of Hydrogen Energy **44**, 4930-4939, doi:10.1016/j.ijhydene.2018.12.185
(2019).